Journal of Cranio-Maxillo-Facial Surgery 54 (2026) 104659

Contents lists available at ScienceDirect

Journal of Cranio-Maxillo-Facial Surgery

journal homepage: www.jcmfs.com

Relative tumour budding (TB rel) predicts occult nodal metastasis, aggressiveness and survival in oral squamous cell carcinoma

J. Peppler [a,b,*,1], C. Cacchi [b,c,1], J. Riese [b,c], A. Klein [b,d], A. Rashad [a,b], K. Wermker [e], O. Vladu [a,b], D. Jonigk [b,c,f], F. Hölzle [a,b], M. Klein [a,b]

[a] Department of Oral & Maxillofacial Surgery, School of Medicine, University Hospital RWTH Aachen, Pauwelsstraße 30, Aachen, 52074, Germany
[b] Center for Integrated Oncology Aachen Bonn Cologne Düsseldorf (CIO ABCD), Aachen, Germany
[c] Institute of Pathology, School of Medicine, University Hospital RWTH Aachen, Pauwelsstraße 30, Aachen, 52074, Germany
[d] Department of Otorhinolaryngology, School of Medicine, University Hospital RWTH Aachen, Pauwelsstrasse 30, Aachen, 52074, Germany
[e] Department of Oral and Cranio-Maxillofacial Surgery, Klinikum Osnabrück GmbH, Am Finkenhügel 1, Osnabrück, 49076, Germany
[f] German Center for Lung Research (DZL), BREATH Hannover, Carl-Neuberg-Str. 1, Hannover, 30625, Germany

ARTICLE INFO

Keywords:
Tumour budding
HNSCC
OSCC
Cancer
Tumour marker
Biomarker

ABSTRACT

Tumour budding (TB) is known as a histopathological parameter defined as single tumour cells or clusters of up to 4 cells at the tumour invasion front (TIF) (TB score 1: 0-4 buds, TB score 2: 5-9 buds, TB score 3: ≥10 buds). However, conventional assessment based on a single section may not capture heterogeneity within the TIF. Therefore, this study applied a novel quantitative approach (TB rel), in which all available sections were evaluated and summarized as an average score. 256 patients with oral squamous cell carcinomas (OSCC) were included and 1289 haematoxylin and eosin-stained sections were analysed. Based on TB rel, patients were stratified into prognostic clusters: Cluster C1 (TB rel = 1.0) and cluster C2 (TB rel >1.0). Increased TB rel was associated with adverse histopathological features reflecting tumour aggression. In clinically node-negative patients (cN0), TB rel identified occult lymph node metastasis (pN+) with an odds ratio of 6.32. Furthermore, patients with higher TB rel showed a higher risk of poorer overall disease progression and survival compared to patients having consistently low TB scores along the TIF. Given its prognostic relevance, TB rel should be integrated into routine diagnostics. This may support more individualized indication for neck dissections.

1. Introduction

Head and neck squamous cell carcinomas (HNSCC) represent the seventh most common cancer entity worldwide, with approximately 890,000 new cases per year worldwide (4.5% of all cancer diagnoses). The overall prognosis remains poor, with around 450,000 deaths annually (4.6% of all cancer-related deaths) (Barsouk et al., 2023). Several studies have demonstrated the association between the presence of lymph node metastases (LNM) with an increased risk of recurrence and distant metastases (DM), as well as increased mortality rates (Leemans et al., 1993, 1994; Dias et al., 2001). Tumour markers could help in the risk stratification and prognosis assessment of HNSCC in order to better evaluate aggressiveness, prognosis, course and lethality (Klein et al., 2021, 2023, Cacchi et al., 2024). To date, no tumour markers have been included in the German clinical guideline for oral squamous cell carcinomas (OSCC) (Deutsche Gesellschaft für Mund-, 2021). A possible candidate for this role could be tumour budding (TB). In other malignant tumours, such as colon carcinoma, TB can be used to assess aggressiveness, prognosis and disease progression (Morodomi et al., 1989; Zlobec et al., 2012, 2014; Puppa et al., 2012; Rogers et al., 2014). Owing to its additional prognostic value, TB analysis has been incorporated in the German colon carcinoma guideline (Deutsche Gesellschaft, 2025). TB is defined as small cell clusters at the tumour invasion front (TIF), consisting of a single cell or clusters of up to 4 tumour cells (Kawachi et al., 2015).

* Corresponding author. Department of Oral & Maxillofacial Surgery, School of Medicine, University Hospital RWTH Aachen, Pauwelsstraße 30, 52074, Aachen, Germany.
E-mail addresses: jpeppler@ukaachen.de (J. Peppler), ccacchi@ukaachen.de (C. Cacchi), jariese@ukaachen.de (J. Riese), anklein@ukaachen.de (A. Klein), arashad@ukaachen.de (A. Rashad), kai.wermker@klinikum-os.de (K. Wermker), ovladu@ukaachen.de (O. Vladu), djonigk@ukaachen.de (D. Jonigk), fhoelzle@ukaachen.de (F. Hölzle), mauklein@ukaachen.de (M. Klein).
[1] Julia Peppler and Claudio Cacchi contributed equally to the study.

https://doi.org/10.1016/j.jcms.2026.104659
Received 18 March 2026; Received in revised form 5 June 2026; Accepted 4 July 2026
Available online 10 August 2026
1010-5182/© 2026 The Authors. Published by Elsevier Ltd on behalf of European Association for Cranio-Maxillo-Facial Surgery. This is an open access article under the CC BY license (http://creativecommons.org/licenses/by/4.0/).

Abbreviation

ASA = American Association of anaesthesiologists
C1/C2 = inferred clusters of tumour budding
DM = distant metastasis
DOI = depth of infiltration
HE = haematoxylin and eosin
HNSCC = head and neck squamous cell carcinoma
HPF = high power field
ITTB rel = intratumoural TB rel
LNM = lymph node metastasis
LNR = lymph node ratio
LSCC = lip squamous cell carcinoma
OSCC = oral squamous cell carcinoma
PTTB rel = peritumoural TB rel
SD = standard deviation
TB = tumour budding
TB rel = tumour budding assessed across all tumour-positive slides of the invasion front
TIF = tumour invasion front
UICC = Union for International Cancer Control

Interestingly for other carcinomas (e.g. breast cancer, lung cancer, urothelial carcinomas, endometrial carcinomas, malignant melanomas), promising studies have reported an association between the presence of TB and poor clinical outcomes (Yamaguchi et al., 2010; Masuda et al., 2012; Okcu et al., 2021, 2023; Lino-Silva et al., 2022; Shi et al., 2023). Different localisations of squamous cell carcinomas have been investigated in the head and neck region (Mäkitie et al., 2019; Mascitti et al., 2023; Tan et al., 2023; Leypold et al., 2025). However, particularly in OSCC, the marked heterogeneity of the TIF distinguishes it from other tumour types. Previously, Cacchi et al. showed that when all sections of the TIF are analysed, TB varies in more than 50% of these sections, indicating that individual positions provide limited information compared with the evaluation of multiple sections. The TB rel method introduced in that study compensates for such intersectional variability, offering a more reliable marker. TB rel represents the mean value of all TB scores distributed across the examined sections of the TIF ($\frac{sum\ of\ all\ TB\ Scores\ across\ the\ TIF}{number\ of\ analysed\ TIF\ sections} = TB_{rel}$) (Cacchi et al., 2024). The optimal number of sections required for a representative TB rel assessment has not yet been determined.

The primary aim of our study was therefore to evaluate the predictive outcome potential of TB rel in a large OSCC cohort of n = 256 patients. The findings indicate that TB rel can be used as a prognostic marker and correlates with an unfavourable clinical outcome. Furthermore, TB rel balances the variability of TB scores across different regions of the TIF. In addition, the study demonstrated that clinically node-negative patients (cN0) with occult lymph node metastasis (pN+) can be detected with TB rel (cN0 but pN+).

2. Materials and methods

2.1. Ethical statement

The study was approved by the local ethics committee (Ethics Committee of the University Hospital RWTH Aachen, approval number EK 22-373) and conducted in accordance with the principles of Good Clinical Practice and the Declaration of Helsinki.

2.2. Patients and clinical data

The study included patients aged over 18 years with histologically confirmed OSCC diagnosed between 2019 and 2023. Patients with a second carcinoma within the HNSCC spectrum or with recurrent disease were also included. The tumour locations included were the floor of the mouth, tongue, buccal mucosa, lower and upper jaw, as well as tumours affecting multiple regions. Oropharyngeal carcinomas were excluded. In case of overlapping location, such as the retromolar area, the most probable origin of the OSCC was determined. All patients underwent preoperative staging, which included at minimum a head and neck computer tomography scan (CT), a magnetic resonance imaging (MRI), a chest X-ray and, when indicated, an abdominal ultrasound. Post-operative and follow-up data, as well as tumour characteristics, were retrospectively retrieved from the hospital information system database. The following clinicopathological parameters were recorded: gender, age at diagnosis, American Association of anaesthesiologists (ASA) score, immunosuppression status, tumour location and extent, presence of second HNSCC, TNM classification including grading, resection margin status, lymphatic vessel, venous and perineural invasion, clinical lymph node status, extra nodal extensions of lymph node metastases, tumour size and depth of infiltration (DOI). The lymph node ratio (LNR) was also determined. The follow-up data included follow-up duration, recurrence, LNM during follow-up, DM during follow-up, overall survival and disease-specific survival.

2.3. Tissue samples and histochemistry

All patients were classified according to the 8th TNM Union for International Cancer Control (UICC) classification (2016) (Brierley et al., 2016). Although the 9th TNM UICC classification (2026) is currently available, the study used the 8th classification, as this was the valid and internationally established one during the patient inclusion period from 2019 to 2023. The histological analyses and the entire histological staining process were performed at the Institute of Pathology, RWTH Aachen University, Germany, following surgical treatment at the Department of Oral and Maxillofacial Surgery, RWTH Aachen University. After defining the patient cohort (2019-2023), formalin-fixed paraffin-embedded (FFPE) sections were provided. The 4 µm thick sections were stained with haematoxylin and eosin (HE) (eosin solution: eosin G solution 1% aqueous; haematoxylin: haematoxylin M (modified according to Mayer)). Staining was performed using the Tissue-Tek Prisma staining machine from Sakura (Umkirch, Germany).

2.4. Analysis of tumour budding in FFPE sections

Two examiners (JP and CC – board-certified pathologist specialized in head and neck pathology) examined the sections for TB in a consensus analysis and were blinded to the clinical data during the evaluation. The 4 µm thick tumour sections were analysed using an Olympus BX51 microscope (Hamburg, Germany, the calibre (diameter) of the 40× eyepiece of the microscope used is 0.55 mm). Digital images of the sections were captured using the NanoZoomer S360MD from Hamamatsu (Herrsching am Ammersee, Germany).

All available FFPE sections for each patient were first reviewed to identify tumour-positive slides. For each section containing the TIF, a representative hot spot was selected under 10× magnification. The TB score was then determined at 20× magnification. One hot spot was evaluated for each tumour-positive section. A distinction was made between intratumoural TB (ITTB) and peritumoural TB (PTTB). ITTB comprised exclusively tumour buds located entirely within the main tumour mass, predominantly within the intratumoural stroma, excluding buds in the vicinity of or at the TIF. Conversely, all tumour buds situated at the TIF and thus outside the main tumour mass were classified as PTTB.

In cases where serial sections were available for the same position, the highest TB score for this position was recorded. Tumour sections with bone tissue that had been previously decalcified were also included. We excluded sections with others staining (for example

Periodic Acid-Schiff (PAS) Staining, Elastic van Gieson).

TB was defined as a single tumour cell or tumour cell cluster of up to 4 cells (Lugli et al., 2017). The FFPE sections were divided into three TB score groups: TB score 1 (0–4 buds = low TB), TB score 2 (5–9 buds = medium TB) and TB score 3 (10 or more buds = high TB). Fig. 1B shows representative microscopic images of the three scores for PTTB and Fig. 1C illustrates the corresponding ITTB categories. The TB scoring procedure followed the methodology described by Xie et al. and Cacchi et al. considering the methodological details outlined above (Xie et al., 2019; Cacchi et al., 2024). Additionally, the TB rel was calculated for each patient by dividing the sum of all TB scores across the TIF by the numbers of analysed TIF sections ($\frac{sum\ of\ all\ TB\ Scores\ across\ the\ TIF}{number\ of\ analysed\ TIF\ sections} = TB_{rel}$), adapted from the study by Cacchi et al. (2024). Based on TB rel, the patient cohort was divided into two clusters: patients with a TB rel of 1.0 were assigned to group C1, showing uniformly low tumour budding (only TB score 1 across all sections). While Group C2 includes patients with TB rel of >1.0, indicating heterogeneity of TB across the TIF with at least one analysed section showing an increased tumour budding score, corresponding to TB score 2 or 3. This binary system was designed to establish a simplified clinical marker. The analytical workflow is illustrated in Fig. 1A.

2.5. Statistical analysis

All analyses were conducted in R version 4.3.3 under RStudio version 2024.04.2. Data visualizations were produced using the pheatmap package for complex heatmaps and ggplot2 (version 3.4) for all other plots. Measures of diversity, specifically Shannon entropy, were calculated using the R entropy package. Saturation (rarefaction) curves and estimation of sampling completeness were derived via the entropart package, using its unbiased estimators and bias-correction methods for Shannon entropy. A generalized linear model with binomial distribution and logit link was fitted to assess whether the association between PTTB cluster and misclassification (cN0 pN+) differed by sampling depth (<9 vs ≥ 9 slides), including an interaction term between cluster and slide number. Inferential statistics were performed as follows: continuous variables that did not meet normality assumptions were compared with the Mann Whitney *U* test, whereas categorical variables were assessed using the Chi-square test or Fisher's exact test, as appropriate for the cell counts. To evaluate the association of various covariates with the risk of cN0 misclassification, we computed odds ratios via logistic regression, adjusting for both continuous and categorical predictors. Survival analysis was carried out using the R survival package: Kaplan-Meier survival curves were estimated with survfit() and group comparisons used the log-rank test. To assess time-varying risk, smoothed hazard rates were estimated nonparametrically with the bshazard package, which fits a B-spline hazard model via generalized linear mixed-model framework. All tests were two-sided, statistical significance was defined as $p < 0.05$.

3. Results

3.1. Patient characteristics

Table 1 and Fig. 2A show an overview of the study population.

3.2. Descriptive parameters

Fig. 2A provides an overview of the study population, presented as a heatmap. In a patient cohort of n = 256 individuals, a total of n = 2654 sections of the primary tumour specimens, which were obtained from surgical resection, were examined. Microscopic analysis revealed that 1333 sections contained parts of the TIF. In total, 1289 sections were evaluated for intratumoural TB rel (ITTB rel) and peritumoural TB rel (PTTB rel). On average, 4.59 sections per patient were assessed for ITTB rel, ranging from 1 to 16 sections. For PTTB rel, the average was 4.87 sections, with a range of 1 to 16. Fig. 2B illustrates the distribution of the number of sections analysed per patient.

3.3. Classification of the patient cohort into two groups

To establish a clinically applicable and robust approach, the patient cohort was divided into two groups based on TB rel, resulting in a binary structure. Group C1 consisted of patients with a TB rel of 1.0 who showed no variability between ITTB and PTTB in the examined sections (only TB score 1 across all sections). Group C2 includes patients with a TB rel value of >1.0. Accordingly, these cases show variability in TB scores across the intratumoural and peritumoural tissue evaluated.

For PTTB rel, n = 169 patients were assigned to Group C1 and n = 84 to Group C2. Regarding ITTB rel, n = 153 patients were classified into Group C1 and n = 83 into Group C2. In total, 33.2% of the evaluated cases exhibited variation in PTTB values among the analysed sections, while 35.17% showed variation in ITTB (Fig. 2C). For better understanding of the relationship between ITTB and PTTB, the distribution of patient cases across clusters C1 and C2 was examined for both parameters. Among n = 233 evaluable cases, 135 cases (57.94%) had both ITTB rel and PTTB rel equal to 1.0, 14 cases (6.01%) had an ITTB rel >1.0 but PTTB rel of 1.0, 15 cases (6.44%) had ITTB rel of 1.0 but PTTB rel >1.0 and 69 cases (29.61%) had both ITTB rel and PTTB rel values greater than 1.0.

Overall, 204 patients (87.55%) were assigned to the same cluster for both ITTB rel and PTTB rel, whereas 29 patients (12.45%) showed discordant cluster classification (Fig. 2D).

3.4. For an accurate representation of tumour heterogeneity, 9 sections (tumour samples) should be assessed

For clinical application, it was of particular interest to determine the number of sections needed to compensate for the variations in TB along the TIF.

Fig. 2E illustrates the distribution of variability among the analysed sections per patient case, revealing a saturation point occurring at nine sections. From this number onwards, the entropy values stabilize, indicating that the heterogeneity of the tumour specimen is accurately represented.

3.5. TB rel correlates with local tumour aggressiveness

Perineural or vascular invasion, as well as the occurrence of lymph node metastases (LNM), are listed in the German HNSCC guideline (version 3.0 - 2021) as indications for postoperative radio chemotherapy due to their association with increased tumour aggressiveness (Deutsche Gesellschaft für Mund-, 2021). Therefore, in the first step, the TB rel clusters were correlated with these factors. In cohort C2, significant associations were observed for extra nodal growth of LNM ($p < 0.001$), lymphatic invasion (L1) ($p = 0.003$), perineural invasion (Pn1) ($p < 0.001$) and venous invasion (V1) ($p = 0.014$) (Fig. 3A). Analysis of lymph node metastases further revealed a significant correlation between the presence of metastases and elevated PTTB rel values in cohort C2 ($p < 0.001$) (Fig. 3B). The ratio of LNM to lymph nodes ($\frac{lymph\ node\ metastasis}{all\ lymph\ nodes} = Lymph\ node\ ratio\ (LNR)$) is also a known poor outcome factor (Chen et al., 2015). Consistently, higher LNR values were also observed in cohort C2 ($p < 0.001$) (Fig. 3C).

Particularly relevant is the evaluation of the clinically node-negative neck (cN0), as 40% of patients with HNSCC have occult metastasis (Deutsche Gesellschaft für Mund-, 2021). Given the observed association between TB rel, LNM and LNR, it was of interest to assess whether TB rel could identify cN0 but pathologically node-positive (pN+) cases.

In this analysis patients in group C2 exhibited a sixfold higher risk (OR 6.32; 95% CI 2.53 – 16.75; $p < 0.001$) of being clinically

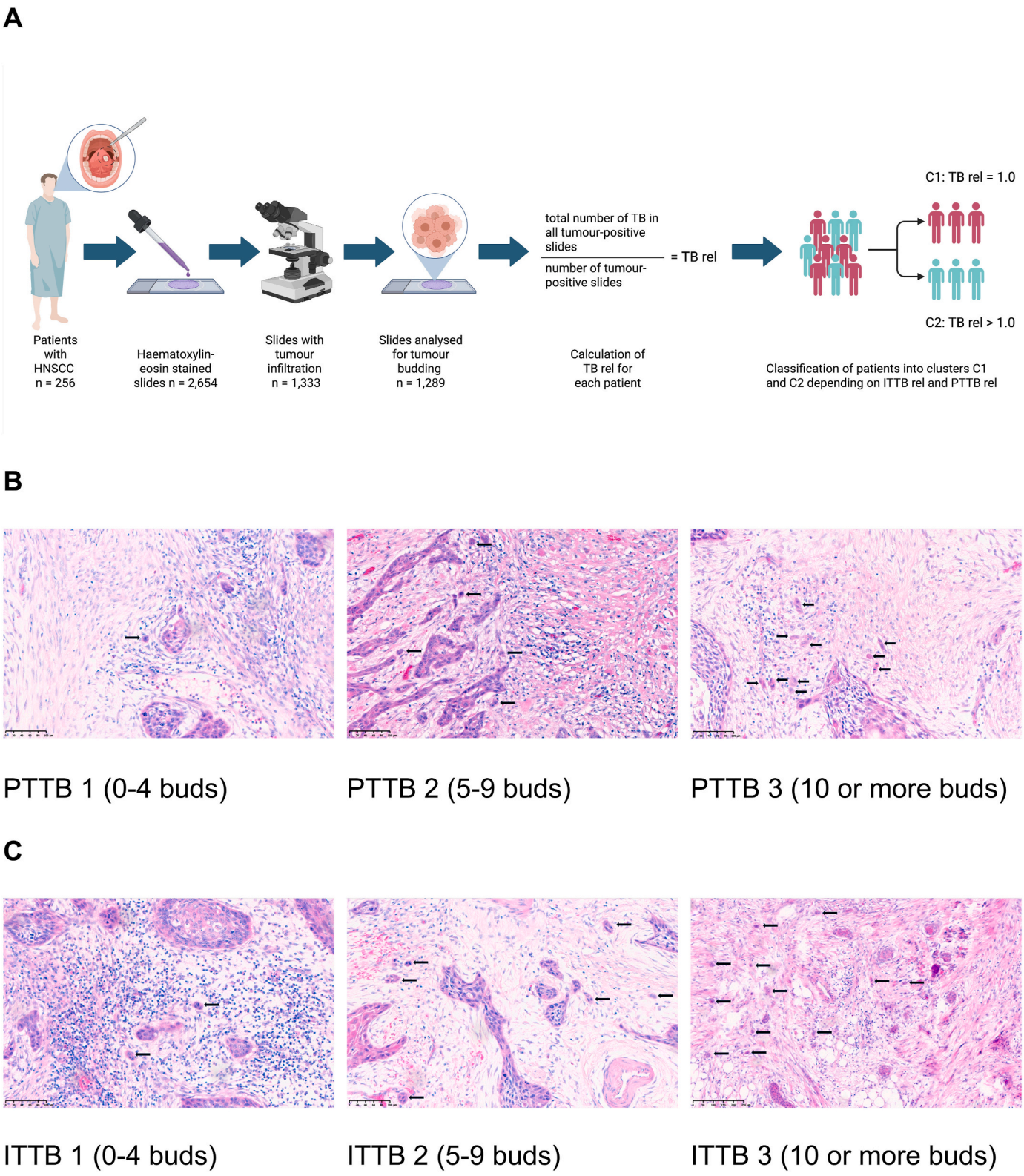


Fig. 1. (**A**) Pictorial representation oft he clinical workflow from sample collection to cluster formation of the patient collective regarding TB rel values. (Created in BioRender. Peppler, J. (2026) https://BioRender.com/46uvbac). (**B**) Representative hotspot of Tumour Budding (TB) in OSCC. Example sections of FFPE-fixed OSCC tissue (HE, magnification 20×) with PTTB. The black arrows show the tumour budding cell nests (≤4 cells). The three tumour budding scores are shown side by side. (**C**) Representative hotspot of Tumour Budding (TB) in OSCC. Microscopic images for ITTB in FFPE-fixed tissue (HE, magnification 20×). Individual tumour buds are indicated by black arrows. The three tumour budding scores are compared side by side.

Table 1
Shows an overview of the patient group in terms of clinical data.

Gender					
Female 130 (50.78%) **Age (years): Mean [range]**			Male 126 (49.22%)		
65.7 [21-92] **ASA-Score**					
ASA 1 15 (5.86%) **Immunosuppression**	ASA 2 114 (44.53%)		ASA 3 123 (48.05%)		ASA 4 4 (1.56%)
No 216 (84.36%) **Localisation**		Mild 37 (14.45%)		Severe 3 (1.17%)	
Floor of mouth 57 (22.27%) **Second primary HNSCC**	Tongue 79 (30.86%)	Buccal mucosa 24 (9.36%)	Upper jaw 55 (21.48%)	Lower jaw 28 (10.94%)	Cross-regional 12 (4.69%)
Yes 39 (15.23%) **Extents of tumour**			No 217 (84.77%)		
Unilateral 215 (83.98%) **Grading**			Bilateral 41 (16.02%)		
G1 14 (5.47%) **T stage**	G2 165 (64.45%)	G2-G3 5 (1.95%)		G3 57 (22.27%)	Not determined 15 (5.89%)
pT1 90 (35.16%) **N stage**	pT2 59 (23.05%)		pT3 42 (16.41%)		pT4 65 (25.39%)
pN0 174 (67.97%) **M stage**	pN1 27 (10.55%)	pN2 20 (7.81%)		pN3 28 (10.94%)	pNx 7 (2.73%)
M0 254 (99.22%) **Lymph vessel invasion**			M1 2 (0.78%)		
L0 218 (85.16%) **Blood vessel invasion**			L1 38 (14.84%)		
V0 227 (88.67%) **Perineural invasion**			V1 29 (11.33%)		
Pn0 161 (62.89%) **Resection status**		Pn1 88 (34.38%)		Pnx 7 (2.73%)	
R0 243 (94.92%) **Extracapsular spread LNM**	R1 8 (3.13%)		R2 0 (0%)		Rx 5 (1.95%)
No 216 (84.38%) **Tumour diameter (mm): Median [range]**		Yes 33 (12.89%)		pNx 7 (2.73%)	
25 [1-125] **Tumour infiltration depth (mm): Median [range]**					
6 [0.2-58] **p16-Status**					
Positive 8 (3.13%) **Clinical lymph node status**		Negative 48 (18.75%)		Not determined 200 (78.16%)	
cN0 190 (74.22%) **Lymph node ratio ($\frac{lymph\ node\ metastasis}{all\ lymph\ nodes} = LNR$): Mean [SD]**			cN+ 66 (25.78%)		
0.0025 [0.088] **Follow up time (months): Mean [range]**					
29.16 [1-77] **Local recurrence**					

(*continued on next page*)

Table 1 (*continued*)

Gender		
No 215 (94.14%) **Lymph node metastasis**	Yes 41 (16.02%)	Mean time (months): Mean [range] 15.28 [2-66]
No 240 (93.75%) **Distant metastasis**	Yes 16 (6.25%)	Mean time (months): Mean [range] 10.38 [3-52]
No 239 (93.36%) **Progress**	Yes 17 (6.64%)	Mean time (months): Mean [range] 10.53 [2-32]
No 209 (81.64%) **Disease specific death**	Yes 47 (18.36%)	Mean time (months): Mean [range] 11.57 [2-66]
No 238 (92.97%)	Yes 18 (7.03%)	

misclassified as negative compared to group C1 (Fig. 3D). To further assess effect strength, a comparison of OR values with other key histomorphological parameters was performed. The most reliable parameter for predicting cN0 but pN + cases was lymphatic vessel invasion (OR 14.43). PTTB rel emerged as the second-strongest predictor (OR 6.32), outperforming ITTB rel (OR 3.23). Depth of infiltration (DOI) showed limited predictive value in our dataset (OR 0.58) (Fig. 3E). To better understand the relationship between TB rel and slide depth we performed a stratified analysis comparing cases with fewer than 9 analysed sections to those with 9 or more sections, corresponding to the empirically observed saturation range. A logistic regression model including an interaction term between TB rel (PTTB cluster) and sampling depth demonstrated a significant association between TB rel and the outcome ($p = 0.00011$), whereas neither sampling depth alone ($p = 0.94$) nor its interaction with TB rel ($p = 0.97$) reached statistical significance. These findings indicate that the prognostic effect of TB rel is stable across different levels of sampling depth and does not significantly differ above or below the saturation threshold (Fig. 3F).

3.6. Elevated TB rel values correlate with disease-specific survival

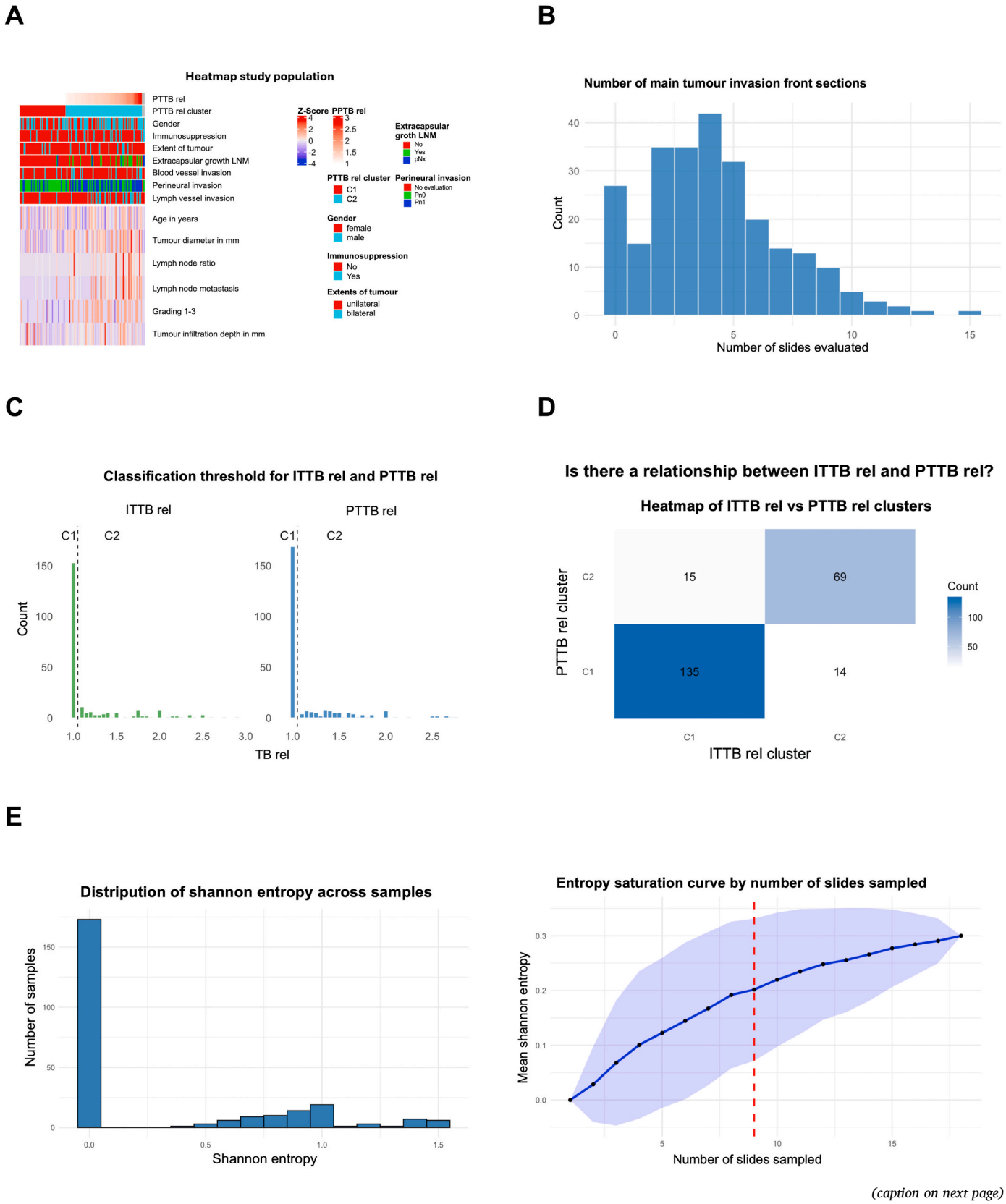
In addition to reflecting local tumour aggression reliably, tumour markers also serve as indicators for disease progression and overall clinical outcome. To evaluate the prognostic relevance of TB rel in a long-term context, follow-up data were analysed for local recurrence, LNM, DM, overall progression, disease-specific survival and disease-specific death. For the individual events (LNM, local recurrence and DM) no statistically significant associations were observed.

However, when these parameters were combined as composite measures of overall progression, a statistically significant difference emerged ($p = 0.019$) between the two groups. Patients in group C1 have a significantly better progression-free survival compared to group C2 (Fig. 4A and 4B). Given the poor 5-year survival rate of approximately 50%, the study further aimed to correlate TB rel with the data on disease-specific survival (Braakhuis et al., 2012). The Kaplan-Meier analysis revealed a highly significant difference between the clusters in terms of survival probability ($p < 0.0001$). The smoothed hazard demonstrated that group C2 has a high hazard at the beginning, which gradually declines over time. The risk was greatest in the first 10-20 months following diagnosis. In contrast, group C1 maintained a consistently low hazard throughout the observation period. Overall, group C2 is characterised by an early elevated risk that decreased overtime but remained consistently higher than that of group C1 (Fig. 4C).

4. Discussion

4.1. Strengths and weaknesses of the study

Our study highlights the importance of analysing multiple regions of a tumour specimen to better reflect tumour heterogeneity using TB rel. The aim was to validate this scoring system with a large patient cohort. Our findings clearly demonstrated that, in most of the cases examined, discrepancies existed within the sections analysed. There are limitations to the study. These include the retrospective design of the study, which allows only limited causal conclusions to be drawn. The follow-up duration varied between patients, due to the inclusion period from 2019 to 2023. Therefore, more recently treated cases had shorter observation periods and results may not fully reflect the long-term outcomes for all patients. Furthermore, the clinical follow-up data were collected retrospectively and may be affected by incomplete documentation. The heterogeneity of the patient cohort and the inclusion of various OSCC subsites represent a realistic clinical picture, which can be considered a strength of this work. Our results indicate that, ideally, 9 sections of a tumour specimen should be evaluated. However, this number could not be achieved in every case. Consequently, tumour heterogeneity may not have been fully represented in every case. Due to the different T stages, some of which have very small tumour diameters, this requirement can only be implemented in clinical practice for larger tumours. In cases such as oral cavity tumours, obtaining nine tissue samples for T2 (2–4 cm) or T3 (>4 cm) lesions is generally feasible for pathology laboratories. This is particularly important when sampling near bone tissue to assess possible infiltration. The use of consensus assessment may be considered a limitation, as the sections were not evaluated independently by two blinded pathologists. However, previous studies have reported good to excellent interobserver and intraobserver agreement for tumour budding, particularly when standardized criteria are applied and the evaluation is performed by experienced or appropriately trained observers. Thus, tumour budding can be regarded as a reproducible histopathological parameter in routine pathological assessment (Boxberg et al., 2019). In the present study, consensus-based evaluation was used to enhance the reliability of the assessment and to reduce potential interobserver variability. The use of consensus analysis of the sections increased the reliability of the results and reduced interobserver variability. The straightforward nature of the evaluation of HE sections allows for standardisation that is easy to reproduce. No complex staining methods are usually required to assess TB rel representatively, making this procedure well suited for use in everyday clinical practice. Moreover, the simplicity and cost-effectiveness of this approach support its potential for widespread global use (Lugli et al., 2017).



(caption on next page)

Fig. 2. Analysis of TB in OSCC (**A**) Heat map showing an overview of the patient cohort depending on the PTTB rel clusters (C1 = red, C2 = blue). Each row represents clinical and histomorphological variables including gender, immunosuppression, tumour extent, extracapsular growth of lymph node metastases, vascular, perineural and lymphatic invasion, age, tumour diameter, lymph node ratio, lymph node metastasis, grading and tumour infiltration depth. Colour intensity reflects Z-scores of the relative PTTB rel values. (**B**) Bar chart illustrates the distribution of the number of tumour invasion front sections examined per patient. Number of evaluated slides per patient is shown on the x-axis; count of patients in whom this number of slides was evaluated is shown on the y-axis. (**C**) The bar chart illustrates the classification of the patient cohort into two clusters (C1 and C2) regarding TB rel (ITTB rel = green; PTTB rel = blue). PTTB cluster C1 n = 169 and cluster C2 n = 84; ITTB rel cluster C1 n = 153 and cluster C2 n = 83. The number of patients is shown on the y-axis, the TB rel value is shown on the x-axis. (**D**) The cross-classified table compares the distribution of TB rel clusters for ITTB and PTTB. Patients in PTTB rel cluster C1 and ITTB rel cluster C1 n = 135, patients in PTTB rel cluster C2 and ITTB rel cluster C2 n = 69, patients in PTTB rel cluster C1 and ITTB rel cluster C2 n = 14 and patients in PTTB rel cluster C2 and ITTB rel cluster C1 n = 15. Colour grading indicates the number of patients in the cluster (darker colour = higher count; lighter colour = smaller count). (**E**) The left side shows a bar chart of the distribution of Shannon entropy across all samples. The number of samples is shown on the y-axis; the Shannon entropy is shown on the x-axis. The right side shows a saturation curve of entropy as a function of the number of sections analysed. The saturation point is reached at 9 sections. The mean Shannon entropy is shown on the y-axis; the number of slides sampled is shown on the x-axis. (For interpretation of the references to colour in this figure legend, the reader is referred to the Web version of this article.)

4.2. TB rel clusters are suitable for predicting tumour aggressiveness, tumour progression and survival

In this study, the patient cohort was divided into two clusters based on TB rel values, allowing for improved clinical comparability, as the risk profiles can be easily derived. The cluster allocation in the present study was based on a highly sensitive threshold, as the presence of a single section with an increased TB score was sufficient to alter risk classification. From a routine diagnostic perspective, this sensitivity may be advantageous, since assessment could theoretically be limited to the number of sections required to identify one section with a TB score of 2 or 3. Once such a section is detected, the patient would be assigned to the higher-risk cluster, irrespective of the TB scores in the remaining sections. Nevertheless, the threshold used in this study should be considered hypothesis-generating and requires validation in further studies before clinical implementation can be recommended. The results of the study show that TB rel more accurately predicts local tumour aggressiveness than disease progression during follow-up. TB rel showed a significant correlation with established parameters of local tumour aggressiveness, including L1, Pn1 and V1. This has also been demonstrated in previous studies (Cacchi et al., 2024; Deshpande et al., 2024; Zanoletti et al., 2024). However, due to intrinsic heterogeneity of the TIF, variability was observed in 33.2% for PTTB and 35.17% for ITTB cases, highlighting the necessity of analysing multiple sections. Cacchi et al. reported comparable findings in a group of n = 66 patients, where analysis of n = 443 sections revealed tumour variability in more than 50% of cases (Cacchi et al., 2024).

The Kaplan-Meier analyses comparing the two TB rel clusters showed no significant difference during follow-up in terms of local recurrence, lymph node metastasis or distant metastasis over time. Nevertheless, a significant correlation could be demonstrated between disease progression and TB rel, despite the absence of significance for individual recurrence-related parameters (recurrence, LNM during follow-up and DM during follow-up). The underlying reason for this discrepancy remains unclear. TB rel may reflect overall tumour aggressiveness, but this association might not be strong enough to influence individual recurrence patterns significantly. This could be due to the complexity of the metastatic process, which depends on multiple biological and microenvironmental factors beyond tumour budding alone.

Regarding tumour-specific survival, the analysis showed significantly poorer overall survival in patients with high TB rel compared with those with low TB rel. The observed survival disadvantage in group C2 is consistent with the results of earlier studies identifying TB as a marker of aggressive tumour behaviour (Wang et al., 2011; Almangush et al., 2018; Panchannavar et al., 2024). This association highlights the prognostic relevance of TB rel in OSCC.

4.3. TB rel variability along the TIF; optimum number of sections and integration into a pathological workflow

Most previous studies on TB in HNSCC have performed analysis based on a representative section or hotspot, rather than systematically examining multiple sections per tumour (Lugli et al., 2017; Joshi et al., 2020; Zlobec et al., 2020; Stogbauer et al., 2023). Compared to other tumour entities, HNSCC exhibits a pronounced degree of heterogeneity (Zhang et al., 2014). With the TB rel we used, a broader range of the TIF was examined, revealing that, in most evaluated cases, differences existed within individual tumours. TB rel can capture this variability and provide a clearer picture of tumour aggressiveness (Cacchi et al., 2024).

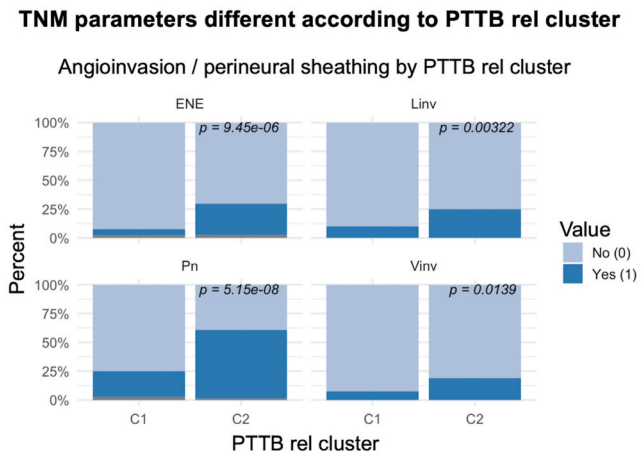
Studies limited to assessing a single section may have overestimated or underestimated the biological behaviour of the tumour. While Shannon entropy analysis indicated a sampling saturation threshold at approximately nine slides, this did not translate into improved predictive performance. The association between PTTB cluster and outcome remained stable across sampling depths, suggesting that the underlying biological signal captured by PTTB clustering is robust to reduced sampling. Thus, while higher slide counts may better capture intratumoral heterogeneity, fewer samples appear sufficient for reliable prediction in this cohort. The number of possible sections depends on tumour size, as it is not possible to obtain this quantity from very small tumours. Therefore, the extent of section evaluation should be adjusted to tumour dimensions, as we discussed above. However, this sampling requirement warrants critical consideration, as our data indicate that the presence of a single section with a TB > 1 is already sufficient to predict a poorer outcome. Far more relevant appears to be the analysis of whether any margin section of the TIF shows a TB Score >1, rather than focusing on a predefined number of sections. This analysis can be easily integrated into clinical workflows, as the HE stained sections are already available for R status evaluation and can thus be used for TB rel assessment.

If validated in further studies, TB rel may represent a promising histopathological marker for risk stratification in OSCC, based on the prognostic value demonstrated in the present study. Although the analysis time per section was not formally recorded in this study, the evaluation of TB on a single section proved to be rapid and efficient, typically requiring approximately 2 min per slide.

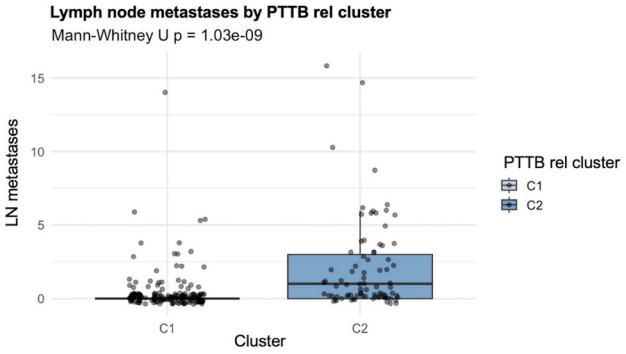
4.4. TB rel analysis could improve the indication for neck dissection in cN0 neck

The current German clinical guideline recommends performing a routine elective neck dissection for patients regardless of T category (Deutsche Gesellschaft für Mund-, 2021). However, patients experience a significant loss of quality of life due to functional limitations and postoperative complaints (Kuntz et al., 1999). The aim should therefore be to perform neck dissection only on patients who appear clinically node-negative but harbour occult metastases, as these patients would derive a clear prognostic benefit from surgical intervention. The results of this study show that TB rel can detect occult metastases in cN0 necks. The study by Leypold et al. identified peritumoural tumour budding as an independent marker for LNM in a cohort of n = 57 patients with lip squamous cell carcinoma (LSCC), demonstrating greater predictive

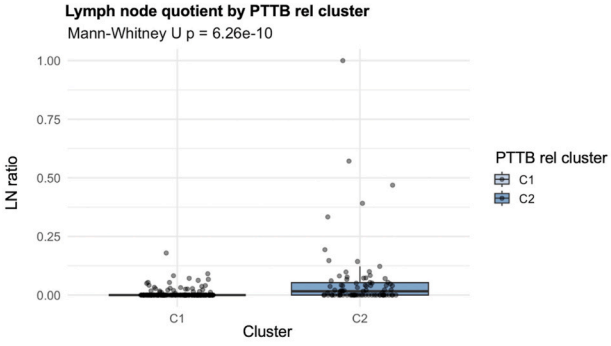
A



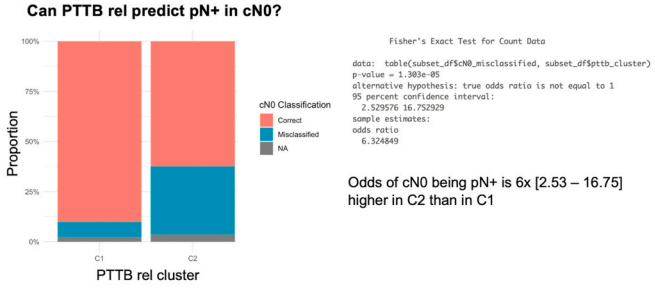
B



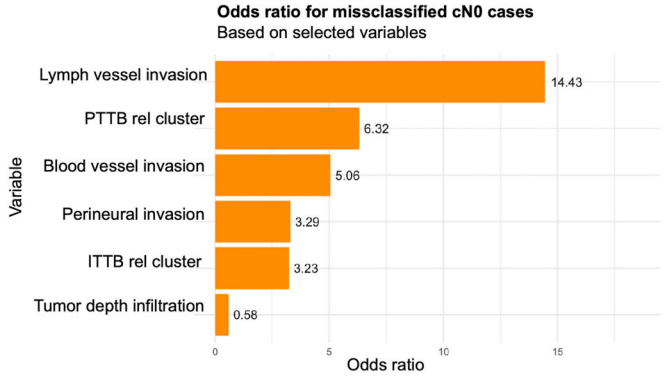
C



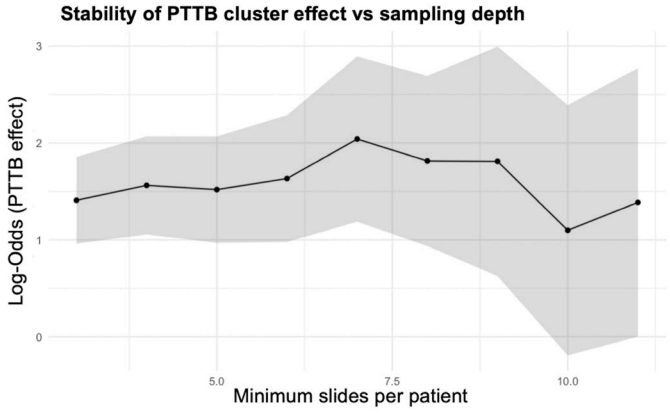
D



E



F



(caption on next page)

Fig. 3. Correlation between PTTB rel clusters and clinical-pathological parameters (**A**) Stacked bar plots illustrate the association of PTTB rel clusters (C1 and C2) with angioinvasion (V1), lymphatic vessel invasion (L1), perineural invasion (Pn1) and extracapsular growth (ENE). Cluster C2 shows a significantly higher rates of ENE ($p < 0.001$), L1 ($p = 0.003$), Pn1 ($p < 0.001$) and V1 ($p = 0.014$). Percentages are displayed on the y-axis, colours indicate absence (light blue) or presence (dark blue) of the respective feature. (**B**) Number of lymph node metastases depending on the PTTB rel cluster (C1, light blue; C2, dark blue). A significant difference is evident for cluster C2 ($p < 0.001$). Number of lymph node metastases is shown on the y-axis. (**C**) Lymph node ratio (LNR) in relation to the PTTB rel clusters (C1, light blue; C2, dark blue). A significant association was observed in cluster C2 ($p < 0.001$). Lymph node quotient is shown on the y-axis. (**D**) Stacked bar plots illustrate the correlation between the PTTB rel cluster (C1 and C2) and pN + status in clinically node-negative (cN0) patients (correct classified, red; misclassified, blue; not determined, grey). The odds ratio shows a 6× [2.53 – 16.75] increased risk for pN+ in cluster C2. Proportion in percentage is shown on the y-axis. (**E**) The bar chart shows the odds ratio of Lymph vessel invasion (14.43), PTTB rel cluster (6.32), Blood vessel invasion (5.06), Perineural invasion (3.29), ITTB rel cluster (3.23) and Tumour depth infiltration (0.58) for predicting misclassifications in cN0 setting. PTTB shows the highest predictive power after lymph vessel invasion. (**F**) The image illustrates the stability of PTTB cluster effect vs sampling depth. Minimum slides per patient are shown on the x-axis, while the y-axis displays the estimated log-odds of the PTTB cluster effect. (For interpretation of the references to colour in this figure legend, the reader is referred to the Web version of this article.)

power than tumour size (Leypold et al., 2025). Pedersen et al. used a semi-automated image analysis algorithm to evaluate TB and demonstrated the correlation of TB with cN0 but pN + necks (Pedersen et al., 2017). However, their study was based on a single tumour sample per case. Therefore, comparisons with studies assessing TB by only a single section of the TIF should take differences in sampling strategy into account, as both the present study and Cacchi et al. observed variability in TB across multiple sections of the TIF (Cacchi et al., 2024).

By clustering TB rel values, it becomes possible to identify patients at increased risk of occult metastasis. Combining TB rel with additional markers capable of detecting such metastases could further improve predictive accuracy. The National Institute for Health and Care Excellence guideline recommends sentinel lymph node biopsy (SLNB) for early stages of oral cancer to rule out metastasis (NICE, 2017). However, SLNB is an invasive procedure, requiring radioisotopes and remains susceptible to false-negative results (Miller et al., 2011). In addition, the cost of the procedure is not negligible. Beyond economic considerations, SLNB is not established as a routine standard procedure according to national guidelines in Germany and therefore cannot be unreservedly recommended in the setting of the present study. In contrast, tumour markers represent a less invasive procedure, as they can be directly determined from the primary tumour specimen. Our results are in line with previous studies showing that L1 is associated with an increased risk of LNM (Doll et al., 2022). Depth of infiltration (DOI) has also been identified as a risk factor for the development of LNM (Mrosk et al., 2024). The current German guideline recommends that elective neck dissection can be omitted in pT1 cN0 carcinoma of the upper jaw if the DOI is less than 3 mm (Deutsche Gesellschaft für Mund-, 2021). Combining DOI with TB rel in a composite score could enhance the predictive value for metastasis. Nevertheless, our data indicate that the effect size of DOI is less pronounced than that of PTTB and L status.

On this basis, it would be possible to weigh up the indication for neck dissection on an individual, potentially reducing over- or under-treatment.

4.5. Integration into a clinical-surgical workflow

In the surgical management of HNSCC, microsurgical free flaps are frequently used for reconstruction (Wong et al., 2010). This involves resecting the tumour, performing a neck dissection with vascular exposure for the anastomosis in the neck, and then inserting the graft for reconstruction. To enable individualized indications for neck dissection based on TB rel findings, a two-stage surgical approach would be required. In the first step, tumour resection would be performed, allowing TB analysis of the TIF across multiple sections. In the second step, the necessity of neck dissection could then be determined. A two-stage procedure can be difficult, especially for larger tumours that require a microvascular graft for reconstruction. Studies have shown that the likelihood of metastasis is higher in T3/T4 tumours compared with smaller T1/T2 tumours (Ludwig et al., 2024). Furthermore, the DOI has been described as a risk factor for metastasis and it is also incorporated into the latest UICC classification of oral cavity carcinomas as a useful parameter for moving from category T1, T2, or T3, regardless of the maximum diameter of the tumour (up to 5 mm, 5 to 10 mm, and greater than 10 mm, respectively) (Brierley et al., 2016; Jangir et al., 2022).

Consequently, such patients are likely to benefit from neck dissections regardless. Based on these considerations, the TB workflow offers advantages, especially for smaller tumours, which could also be treated with local reconstruction or through a delayed reconstructive approach. In some cases, performing only vascular exposure without immediate neck dissection may be beneficial, as it helps to avoid persistent postoperative oedema. Patients can thus benefit from a shorter operation time and a shorter hospital stay (Douglas et al., 2023). Nevertheless, neck dissection as a second operation should ideally be avoided after vascular exposure and microvascular anastomosis to minimize the risk of compromising the anastomosis or the transplanted flap. In addition to surgical therapy, radio- or radio chemotherapy remain important modalities for HNSCC, including adjuvant options following surgical tumour resection. Indications for radio(chemo)therapy include perineural or vascular invasion and extracapsular growth of LNM (Deutsche Gesellschaft für Mund-, 2021). These are histomorphological characteristics of the tumour that can be determined on HE sections and directly influence therapeutic decisions.

Further studies could therefore focus on exploring the potential of TB rel clusters as an additional histomorphological marker to predict treatment response to radiotherapy and/or system therapy.

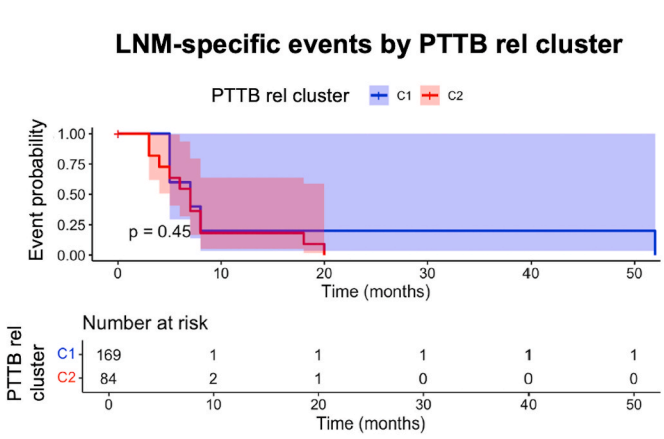
4.6. Integration into neoadjuvant immunotherapy

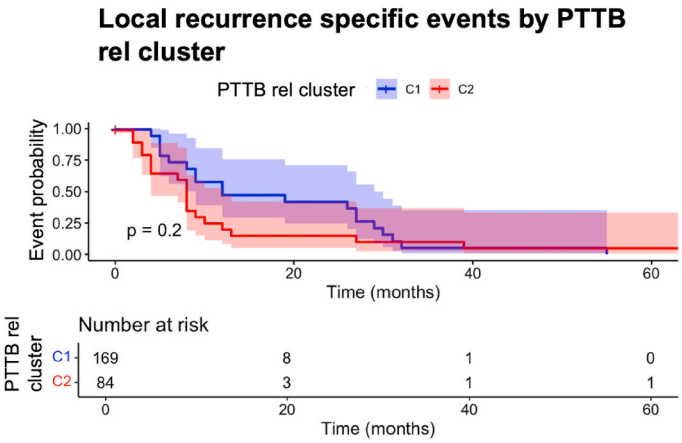
A recently emerging concept in the treatment of HNSCC is neoadjuvant immunotherapy with pembrolizumab. In the study by Uppaluri et al., patients received pembrolizumab in addition to standard therapy, both before and after surgery. The pembrolizumab-treated group showed significantly better event-free survival compared to the control group (Uppaluri et al., 2025). Considering our research on TB rel, this two-stage therapeutic concept can also be integrated into a workflow that incorporates immunotherapy. In such an approach, neoadjuvant immunotherapy would be initiated first, followed by tumour resection an TB rel analysis, and finally, an optional neck dissection and reconstructive procedure. From a biological perspective, this sequence would enable prolonged antigen presentation within the lymph nodes and thus potentially enhance the immunological response (Zhong et al., 2024) (Payne et al., 2024).

5. Conclusion

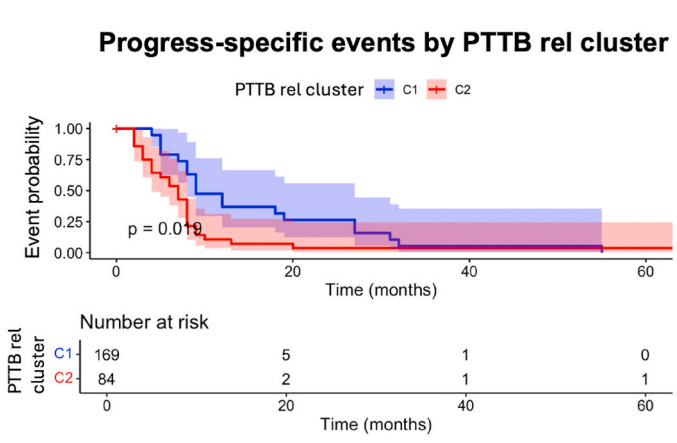
Prospective, multicentre studies appear necessary in the future to validate the prognostic role of TB rel in OSCC. To enhance risk stratification, a combination of several markers such as TB rel, DOI and L1 should be considered. Additionally, the morphological evaluation of the tumour cells that make up the buds is particularly interesting, especially regarding their interaction with the cells of the peritumoural stroma. Furthermore, it would be of interest to evaluate the influence of TB rel clusters on the response to forms of therapy such as radio(chemo)therapy. In the long term, TB rel could contribute to individualized

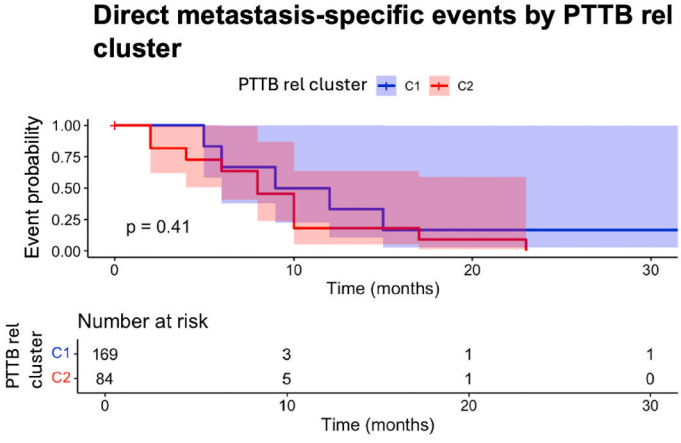
A



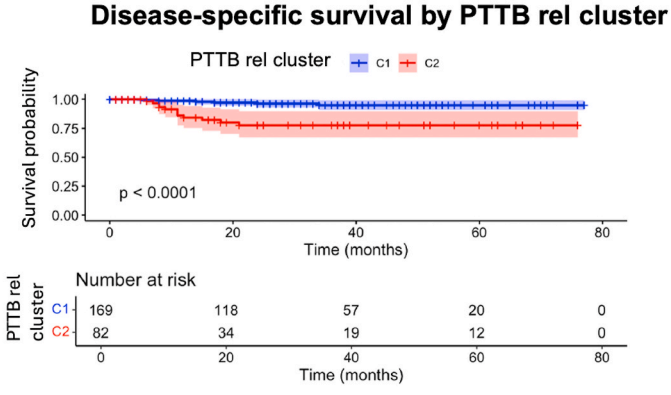


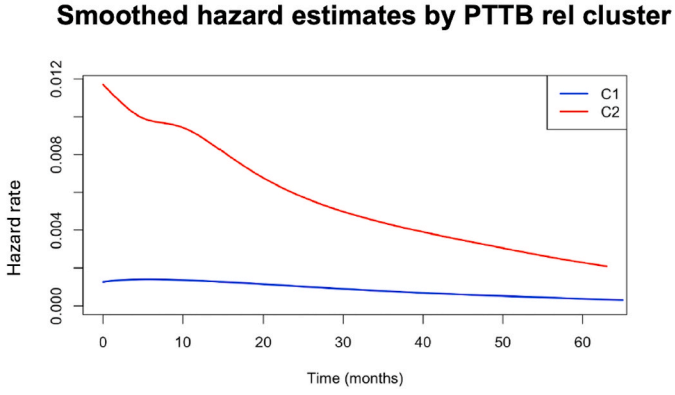
B





C





(caption on next page)

Fig. 4. Event- and survival-specific analyses stratified by PTTB rel clusters. (**A**) Event-free survival probability for locoregional recurrence (LocRec) and lymph node-specific events (LNM) during follow-up according to PTTB cluster (C1, blue; C2 red). No significant difference between the clusters is apparent LNM ($p = 0.45$) and LocRec ($p = 0.2$). Shaded areas represent 95% confidence intervals. Below each plot the number of patients at risk is shown. (**B**) Kaplan-Meier curve for progression-specific events and distant metastases (DM) depending on PTTB rel clusters (C1, blue; C2, red). No significant difference between the clusters was found for distant metastasis ($p = 0.41$). A significant correlation was found for C2 in terms of progression ($p = 0.019$). Shaded areas represent 95% confidence intervals. Below each plot the number of patients at risk is shown. (**C**) The left side shows disease-specific survival after PTTB rel Cluster (C1, blue; C2, red) with significantly worse outcome in cluster C2 ($p < 0.0001$). The number of patients at risk is shown below the Kaplan-Meier curve. The right side shows a smoothed hazard ratio for both clusters (C1, blue; C2, red) over time with consistently higher rates for C2. (For interpretation of the references to colour in this figure legend, the reader is referred to the Web version of this article.)

indication for neck dissections based on the estimated risk of occult metastasis.

Authors contributions

JP analysed the histology, selected and developed the photos of the histological sections, performed data acquisition, interpreted data, conducted literature search and wrote the manuscript. CC analysed the histology, supervised and selected the slides for the photos of the histological sections, contributed to study conception and critically revised the manuscript. MK supervised, contributed to study conception and revised the manuscript. DJ directed (histo)pathological work-up, provided infrastructure, made histological slides available, gave important intellectual input and critically revised the manuscript. MK and JR interpreted data. JR, AK, AR, KW, OV and FH gave important intellectual input and critically revised the manuscript. All authors read and approved the final manuscript.

Declaration of Ai And Ai-Assisted technologies in the manuscript preparation process

Generative AI and AI-assisted technologies were NOT used in the preparation of this work.

Declaration of interest

None.

Acknowledgements

We sincerely thank the whole team of the Institute of Pathology and Department of Oral & Maxillofacial Surgery at RWTH Aachen University. The schematic illustration in Fig. 1A was created in BioRender.com and is reproduced under a valid publication licence (Peppler, J. (2026) https://BioRender.com/46uvbac). This work was supported by a grant of Stiftung Tumorforschung Kopf-Hals awarded to JR.

References

Almangush, A., Pirinen, M., Heikkinen, I., Mäkitie, A.A., Salo, T., Leivo, I., 2018. Tumour budding in oral squamous cell carcinoma: a meta-analysis. Br. J. Cancer 118, 577–586.

Barsouk, A., Aluru, J.S., Rawla, P., Saginala, K., Barsouk, A., 2023. Epidemiology, risk factors, and prevention of head and neck squamous cell carcinoma. Med. Sci. 11.

Boxberg, M., Bollwein, C., Jöhrens, K., Kuhn, P.H., Haller, B., Steiger, K., Wolff, K.D., Kolk, A., Jesinghaus, M., Weichert, W., 2019. Novel prognostic histopathological grading system in oral squamous cell carcinoma based on tumour budding and cell nest size shows high interobserver and intraobserver concordance. J. Clin. Pathol. 72, 285–294.

Braakhuis, B.J., Brakenhoff, R.H., Leemans, C.R., 2012. Treatment choice for locally advanced head and neck cancers on the basis of risk factors: biological risk factors. Ann. Oncol. 23 (Suppl. 10), x173–x177.

Brierley JD, Gospodarowicz MK, Wittekind C: TNM Classification of Malignant Tumours, eighth edition.

Cacchi, C., Fischer, H.J., Wermker, K., Rashad, A., Jonigk, D.D., Hölzle, F., Klein, M., 2024. New tumor budding evaluation in head and neck squamous cell carcinomas. Cancers (Basel) 16.

Chen, C.C., Lin, J.C., Chen, K.W., 2015. Lymph node ratio as a prognostic factor in head and neck cancer patients. Radiat. Oncol. 10, 181.

Deshpande, N.S., Munemane, A.B., Karle, R.R., Dongre, S.D., 2024. Relevance of tumor budding and pattern of invasion in oral squamous cell carcinoma. Int. J. Appl. Basic Med. Res. 14, 29–34.

Deutsche Gesellschaft für Mund- K-uGD: S3-Leitlinie Diagnostik und Therapie des Mundhöhlenkarzinoms, Version 3.0 (AWMF-Register-Nr. 007-100OL), 2021. Arbeitsgemeinschaft der Wissenschaftlichen Medizinischen Fachgesellschaften (AWMF). https://register.awmf.org/assets/guidelines/007-100Olk_S3-Diagnostik-Therapie-Mundhoehlenkarzinom_2021-03-abgelaufen.pdf.

Deutsche Gesellschaft für Gastroenterologie V-uSD: S3-Leitlinie Kolorektales Karzinom, Version 3.2 (AWMF-Register-Nr. 021-007OL), 2025. Arbeitsgemeinschaft der Wissenschaftlichen Medizinischen Fachgesellschaften (AWMF). https://register.awmf.org/assets/guidelines/021-007Oll_S3_Kolorektales-Karzinom_2026-03_1.pdf.

Dias, F.L., Kligerman, J., Matos, de Sá G., Arcuri, R.A., Freitas, E.Q., Farias, T., Matos, F., Lima, R.A., 2001. Elective neck dissection versus observation in stage I squamous cell carcinomas of the tongue and floor of the mouth. Otolaryngol. Head Neck Surg. 125, 23–29.

Doll, C., Mrosk, F., Wuester, J., Runge, A.S., Neumann, F., Rubarth, K., Heiland, M., Kreutzer, K., Voss, J., Raguse, J.D., Koerdt, S., 2022. Pattern of cervical lymph node metastases in squamous cell carcinoma of the upper oral cavity - how to manage the neck. Oral Oncol. 130, 105898.

Douglas, C., Hewitt, L., Yabe, T.E., Mitchell, J., Ashford, B., 2023. Quality of life impacts following surgery for advanced head and neck cancer. World J. Oncol. 14, 150–157.

Jangir, N.K., Singh, A., Jain, P., Khemka, S., 2022. The predictive value of depth of invasion and tumor size on risk of neck node metastasis in squamous cell carcinoma of the oral cavity: a prospective study. J. Cancer Res. Therapeut. 18, 977–983.

Joshi, P., Pol, J., Chougule, M., Jadhav, K., Patil, S., Patil, S., 2020. Tumor budding - a promising prognostic histopathological parameter in oral squamous cell carcinoma - a comparative immunohistochemical study. J. Oral Maxillofac. Pathol. 24, 587.

Kawachi, H., Eishi, Y., Ueno, H., Nemoto, T., Fujimori, T., Iwashita, A., Ajioka, Y., Ochiai, A., Ishiguro, S., Shimoda, T., Mochizuki, H., Kato, Y., Watanabe, H., Koike, M., Sugihara, K., 2015. A three-tier classification system based on the depth of submucosal invasion and budding/sprouting can improve the treatment strategy for T1 colorectal cancer: a retrospective multicenter study. Mod. Pathol. 28, 872–879.

Klein, M., Wefers, M., Hallermann, C., Fischer, H.J., Hölzle, F., Wermker, K., 2023. IMP3 expression as a potential tumour marker in high-risk localisations of cutaneous squamous cell carcinoma: IMP3 in metastatic cSCC. Cancers (Basel) 15.

Klein, M., Wermker, K., Hallermann, C., Pannier, F., Hölzle, F., Modabber, A., 2021. Immune checkpoint analysis in lip cancer. J. Craniomaxillofac. Surg. 49, 950–958.

Kuntz, A.L., Weymuller Jr., E.A., 1999. Impact of neck dissection on quality of life. Laryngoscope 109, 1334–1338.

Leemans, C.R., Tiwari, R., Nauta, J.J., van der Waal, I., Snow, G.B., 1993. Regional lymph node involvement and its significance in the development of distant metastases in head and neck carcinoma. Cancer 71, 452–456.

Leemans, C.R., Tiwari, R., Nauta, J.J., van der Waal, I., Snow, G.B., 1994. Recurrence at the primary site in head and neck cancer and the significance of neck lymph node metastases as a prognostic factor. Cancer 73, 187–190.

Leypold, S., Riese, J., Cacchi, C., Wermker, K., Vladu, O., Jonigk, D., Hölzle, F., Klein, M., 2025. Tumor budding predicts lymph node metastasis in squamous cell carcinoma of the lip. Head Face Med. 21 (74).

Lino-Silva, L.S., Zepeda-Najar, C., Caro-Sánchez, C.H., Herrera-Gómez, Á., Salcedo-Hernández, R.A., 2022. Prognostic significance of tumor budding in melanoma. Melanoma Res. 32, 318–323.

Ludwig, R., Werlen, S., Barbatei, D., Widmer, L., Pouymayou, B., Balermpas, P., Elicin, O., Dettmer, M., Zrounba, P., Giger, R., Grégoire, V., Schubert, A., Unkelbach, J., 2024. Patterns of lymph node involvement for oral cavity squamous cell carcinoma. Radiother. Oncol. 200, 110474.

Lugli, A., Kirsch, R., Ajioka, Y., Bosman, F., Cathomas, G., Dawson, H., El Zimaity, H., Fléjou, J.F., Hansen, T.P., Hartmann, A., Kakar, S., Langner, C., Nagtegaal, I., Puppa, G., Riddell, R., Ristimäki, A., Sheahan, K., Smyrk, T., Sugihara, K., Terris, B., Ueno, H., Vieth, M., Zlobec, I., Quirke, P., 2017. Recommendations for reporting tumor budding in colorectal cancer based on the International Tumor Budding Consensus Conference (ITBCC) 2016. Mod. Pathol. 30, 1299–1311.

Mascitti, M., Togni, L., Caponio, V.C.A., Zhurakivska, K., Lo Muzio, L., Rubini, C., Santarelli, A., Troiano, G., 2023. Prognostic significance of tumor budding thresholds in oral tongue squamous cell carcinoma. Oral Dis. 29, 1947–1958.

Masuda, R., Kijima, H., Imamura, N., Aruga, N., Nakamura, Y., Masuda, D., Takeichi, H., Kato, N., Nakagawa, T., Tanaka, M., Inokuchi, S., Iwazaki, M., 2012. Tumor budding is a significant indicator of a poor prognosis in lung squamous cell carcinoma patients. Mol. Med. Rep. 6, 937–943.

Miller, M.W., Vetto, J.T., Monroe, M.M., Weerasinghe, R., Andersen, P.E., Gross, N.D., 2011. False-negative sentinel lymph node biopsy in head and neck melanoma. Otolaryngol. Head Neck Surg. 145, 606–611.

Mäkitie, A.A., Almangush, A., Rodrigo, J.P., Ferlito, A., Leivo, I., 2019. Hallmarks of cancer: tumor budding as a sign of invasion and metastasis in head and neck cancer. Head Neck 41, 3712–3718.

Morodomi, T., Isomoto, H., Shirouzu, K., Kakegawa, K., Irie, K., Morimatsu, M., 1989. An index for estimating the probability of lymph node metastasis in rectal cancers. Lymph node metastasis and the histopathology of actively invasive regions of cancer. Cancer 63, 539–543.

Mrosk, F., Krom, V., Doll, C., Mödl, L., Kreutzer, K., Voss, J., Rendenbach, C., Heiland, M., Koerdt, S., 2024. Prediction of nodal disease in oral squamous cell carcinoma of the tongue: histopathological risk assessment with the focus on depth of invasion. Clin. Oral Invest. 28, 466.

National Institute for Health and Care Excellence (NICE), 2017. Head and neck cancer. https://www.nice.org.uk/guidance/qs146/resources/head-and-neck-cancer-pdf-75545482867909. London, UK.

Okcu, O., Öztürk, Ç., Şen, B., Arpa, M., Bedir, R., 2021. Tumor budding is a reliable predictor for death and metastasis in invasive ductal breast cancer and correlates with other prognostic clinicopathological parameters. Ann. Diagn. Pathol. 54, 151792.

Okcu, O., Şen, B., Aşkan, G., Öztürk, Ç., Öztürk, S.D., Bedir, R., 2023. Tumor budding is an independent prognostic factor to predict overall survival in endometrial endometrioid carcinoma: a retrospective study. Int. J. Surg. Pathol. 31, 26–37.

Panchannavar, G.S., Angadi, P.V., 2024. Tumor budding is a prognostic marker for overall survival and not for lymph node metastasis in oral squamous cell carcinoma - systematic review update and meta-analysis. J. Oral Biol. Craniofac. Res. 14, 362–369.

Payne, K., Nenclares, P., Schilling, C., 2024. The impact of elective cervical lymph node treatment on the tumour immune response in head and neck squamous cell carcinoma: time for a change in treatment strategy? BJC Rep. 2, 68.

Pedersen, N.J., Jensen, D.H., Lelkaitis, G., Kiss, K., Charabi, B., Specht, L., von Buchwald, C., 2017. Construction of a pathological risk model of occult lymph node metastases for prognostication by semi-automated image analysis of tumor budding in early-stage oral squamous cell carcinoma. Oncotarget 8, 18227–18237.

Puppa, G., Senore, C., Sheahan, K., Vieth, M., Lugli, A., Zlobec, I., Pecori, S., Wang, L.M., Langner, C., Mitomi, H., Nakamura, T., Watanabe, M., Ueno, H., Chasle, J., Conley, S.A., Herlin, P., Lauwers, G.Y., Risio, M., 2012. Diagnostic reproducibility of tumour budding in colorectal cancer: a multicentre, multinational study using virtual microscopy. Histopathology 61, 562–575.

Rogers, A.C., Gibbons, D., Hanly, A.M., Hyland, J.M., O'Connell, P.R., Winter, D.C., Sheahan, K., 2014. Prognostic significance of tumor budding in rectal cancer biopsies before neoadjuvant therapy. Mod. Pathol. 27, 156–162.

Shi, R., Le Tan, M.T., Lim, G.H., Du, J., Zhang, L., Zeng, L., Tan, P.H., 2023. Prognostic value of tumor budding in urothelial carcinoma: a meta-analysis and systematic review. Lab. Invest. 103, 100136.

Stogbauer, F., Beck, S., Ourailidis, I., Hess, J., Poremba, C., Lauterbach, M., Wollenberg, B., Buchberger, A.M.S., Jesinghaus, M., Schirmacher, P., Stenzinger, A., Weichert, W., Boxberg, M., Budczies, J., 2023. Tumour budding-based grading as independent prognostic biomarker in HPV-positive and HPV-negative head and neck cancer. Br. J. Cancer 128, 2295–2306.

Tan, A., Taskin, T., 2023. Tumor budding should be in oral cavity cancer reporting: a retrospective cohort study based on tumor microenvironment. Cancers (Basel) 15.

Uppaluri, R., Haddad, R.I., Tao, Y., Le Tourneau, C., Lee, N.Y., Westra, W., Chernock, R., Tahara, M., Harrington, K.J., Klochikhin, A.L., Braña, I., Vasconcelos Alves, G., Hughes, B.G.M., Oliva, M., Pinto Figueiredo Lima, I., Ueda, T., Rutkowski, T., Schroeder, U., Mauz, P.S., Fuereder, T., Laban, S., Oridate, N., Popovtzer, A., Mach, N., Korobko, Y., Costa, D.A., Hooda-Nehra, A., Rodriguez, C.P., Bell, R.B., Manschot, C., Benjamin, K., Gumuscu, B., Adkins, D., 2025. Neoadjuvant and adjuvant pembrolizumab in locally advanced head and neck cancer. N. Engl. J. Med. 393, 37–50.

Wang, C., Huang, H., Huang, Z., Wang, A., Chen, X., Huang, L., Zhou, X., Liu, X., 2011. Tumor budding correlates with poor prognosis and epithelial-mesenchymal transition in tongue squamous cell carcinoma. J. Oral Pathol. Med. 40, 545–551.

Wong, C.H., Wei, F.C., 2010. Microsurgical free flap in head and neck reconstruction. Head Neck 32, 1236–1245.

Xie, N., Yu, P., Liu, H., Liu, X., Hou, J., Chen, X., Huang, H., Wang, C., 2019. Validation of the international tumor budding consensus conference (2016) recommendations in oral tongue squamous cell carcinoma. J. Oral Pathol. Med. 48, 451–458.

Yamaguchi, Y., Ishii, G., Kojima, M., Yoh, K., Otsuka, H., Otaki, Y., Aokage, K., Yanagi, S., Nagai, K., Nishiwaki, Y., Ochiai, A., 2010. Histopathologic features of the tumor budding in adenocarcinoma of the lung: tumor budding as an index to predict the potential aggressiveness. J. Thorac. Oncol. 5, 1361–1368.

Zanoletti, E., Daloiso, A., Nicolè, L., Cazzador, D., Mondello, T., Franz, L., Astolfi, L., Marioni, G., 2024. Tumor budding to investigate local invasion, metastasis, and prognosis of head and neck carcinoma: a systematic review. Head Neck 46, 651–671.

Zhang, P., Mirani, N., Baisre, A., Fernandes, H., 2014. Molecular heterogeneity of head and neck squamous cell carcinoma defined by next-generation sequencing. Am. J. Pathol. 184, 1323–1330.

Zhong, N.N., Liu, B., Bu, L.L., 2024. Neoadjuvant immunotherapy: new horizon for lymph node preservation. MedComm 5, e577–e2024.

Zlobec, I., Berger, M.D., Lugli, A., 2020. Tumour budding and its clinical implications in gastrointestinal cancers. Br. J. Cancer 123, 700–708.

Zlobec, I., Borner, M., Lugli, A., Inderbitzin, D., 2012. Role of intra- and peritumoral budding in the interdisciplinary management of rectal cancer patients. Int. J. Surg. Oncol., 795945, 2012.

Zlobec, I., Hädrich, M., Dawson, H., Koelzer, V.H., Borner, M., Mallaev, M., Schnüriger, B., Inderbitzin, D., Lugli, A., 2014. Intratumoural budding (ITB) in preoperative biopsies predicts the presence of lymph node and distant metastases in colon and rectal cancer patients. Br. J. Cancer 110, 1008–1013.